PV FED MODULAR MULTILEVEL INVERTER WITH PI AND FUZZY CONTROL FOR MARINE WATER PUMPING APPLICATIONS

P. K. Dhal[1], Dakyrmen Kongri[1], Vempalle Rafi[2] and S. Vinoth John Prakash[1]
[1]Department of Electrical and Electronics Engineering, Vel Tech Rangarajan Dr. Sagunthala R & D Institute of Science and Technology, Chennai, India
[2]Department of EEE, JNTUA College of Engineering Pulivendula, Kadapa, India
E-Mail: vempallerafi@gmail.com

ABSTRACT

In this paper, we describe the outcomes of our investigation into the design and construction of a modular multilevel inverter (MMI) using intelligent control approaches to manage the induction motor (IM) drive in marine water pumping applications. Specifically, we were interested in controlling the speed of the IM. The multi-model input multi-output (MMI-IM) drive coupled with a fuzzy logic controller is used in the solution that has been suggested. A range of robustness measurements, including as peak overshoot, inverter settling time, and total harmonic distortion (THD), are used to assess the performance of the controllers. The intelligent controller, IM drive, and MMI are all components of the suggested control approach for water pumping applications that are used in the marine industry. To enhance both the efficiency and usefulness of the system, the methodology that has been suggested makes use of several intelligent control strategies. This is the aspect that sets it apart from other methods.

Keywords: fuzzy logic, induction motor drive, modular multilevel inverter, proportional-integral, total harmonic distortion.

Manuscript Received 29 August 2023; Revised 20 November 2023; Published 11 December 2023

1. INTRODUCTION

The nautical and shipping sectors have contributed to a worldwide decrease in air pollution and energy consumption. To reduce accidental and marine pollution, the International Convention for the Prevention of Pollution from Ships (MARPOL) established regulations [1, 2]. Marine diesel engines account for 3 percent of global CO2 emissions from shipping related to climate change [3]. Diesel engines used in maritime transportation emit some of the most harmful pollutants into the atmosphere. The UNFCCC and IMO studied and created shipping industry CO2 emission reduction requirements. Depletion of traditional energy sources is causing a global energy crisis and air and water pollution. Ship diesel engines emit greenhouse gases and CO2 [3], [4]. The shipping industry adopted solar electricity to reduce environmental pollution. Despite a growing global population and need for electrical power, solar energy and inverter power quality are needed [3], [4]. Conventional energy sources are dwindling, leading to a worldwide energy crisis. Global warming is being triggered by the greenhouse effect. This century's earth surface temperature is anticipated to rise 3C to 6C [4], [5].

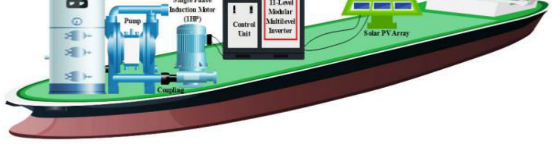

Figure-1. The 11-level inverter design schematic.

Solar energy is perfect for residential and maritime applications due to its silent operation (no moving parts) and small footprint (ship roofing). Ships are now equipped with solar photovoltaics to reduce their carbon footprint and produce power. Power electronic converters and inverters are used to transform the solar energy and then send it on to multiple high-power loads [6]. Ships of the present day are looking at integrated power converters that can function on renewable energy sources. Voltage and frequency changes in power converters lead to harmonic distortions [7, 8]. 70% of a ship's electricity goes towards powering the pumps [9, 10]. The converter, a vital component of the ship's power electronics, operates the motors, although it is susceptible to harmonics. Modular inverters with a smart controller may lower harmonics and boost power quality aboard ships. The study presents a symmetric multilevel module that, without additional circuitry, can create negative voltage levels. Solar-powered, eleven-stage inverter with fine-tuned control is shown in Figure-1. A variable frequency motor driven by an inverter operates the seawater cooling pumps on board. The multilayer inverter-fed IM drive is analyzed using PI and FLC controllers. Since the proportional-integral (PI) controller has a low maximum peak overshoot and is very stable, it is often employed for speed regulation. FLCs are the simplest and most clever controllers for controlling the speed of an induction motor. Ships' water pumps run nonstop. The inverter controls the starting current and supply voltage of an induction motor. Commutation issues plague DC motors. DC motors have drawbacks, thus ships favour induction motors. Seawater pumps well and cools freshwater. MMI topology is used in sustained control approaches for single-phase IM drives for maritime water pumping [11]. Maximum solar power extraction in air

ARPN Journal of Engineering and Applied Sciences

circumstances governs real-time speed control. To adjust the induction motor speed, the inverter progressively changes the switching frequency. Optimized Pulse Width Modulation (PWM) created by a FL controller modulating signal improves power quality.

2. STRATEGY FOR SYSTEM SETUP AND MANAGEMENT

According to the rating of the IM drive linked water pump, a maximum PV array power output of 150W is considered under Standard Test Conditions (STC) (1000W/m2, 25C). With the help of a modular multilevel inverter [11], [12], the working power capacity of the PV array is chosen to power the motor pump system.

A. Design of PV

Arrays 36 solar PV cells (36 x 0.688 V = 24.7Voc) are used to create a 10W solar PV module. The maximum power is 10Wp, the operating voltage is 21.6V, and the short-circuit current is 0.659 A. Modules can handle up to 17V and 0.588A of current, respectively (Pmax = Vmp Imp = 17 0.588= 9.96W). As the power source, we employ a 72-cell solar module connected in series, capable of producing 20W. The maximum power is 20Wp, the operating voltage is 21.5V, and the short-circuit current is 1.24 A. At Vmp = 17.8V and Imp =1.142A, a module's maximum power output (Pmax = Vmp Imp = 17 1.14 = 19.38W) is reached. By connecting the two different power ratings in series and parallel, we may reach the greater power capacity of 150 W at STC (5 x 10 = 50W, 5 x 20 = 100W). Equation (1), which describes the current through a solar cell, imposes four unknown limitations on the solution space that must be met to achieve the V-I characteristics of a PV cell [13], [14].

$$I = I_L - I_D = I_L - I_O \; e^{\frac{(V+R_S)}{s}} - 1 \qquad (1)$$

a) Calculation of Light Current (IL)

The formula for calculating an approximation of the illuminant current, I_L, is,

$$I_L = \frac{\phi}{\phi_{ref}}\left[I_{L,ref} + \mu_{1,SC}\left(T_C - T_{c,ref}\right)\right] \qquad (2)$$

b) Calculation of Saturation Current (I_0)

Saturation current can be calculated as

$$I_o = I_{o,ref}\left(\frac{T_{c,ref}+273}{T_c+273}\right)^3 \exp\left[\frac{e_{gap}N_s}{q\propto_{ref}}\left(1 - \frac{T_{c,ref}+273}{T_c+273}\right)\right] \qquad (3)$$

Saturation current under the reference situation can be calculated as,

$$I_{o,ref} = I_{L,ref} \exp\left(-\frac{V_{oc,ref}}{\propto_{ref}}\right) \qquad (4)$$

c) Calculation of TVTC Factor

The task of temperature is reflected in the TVTC factor (α), also known as the Thermal Voltage Timing Completion factor.

$$\propto_{ref} = \frac{2V_{mp,ref} - V_{oc,ref}}{\frac{I_{sc,ref}}{I_{sc,ref}-I_{mp,ref}} + \ln\left(1 - \frac{I_{mp,ref}}{I_{sc,ref}}\right)} \qquad (5)$$

$$\propto = \frac{T_C+273}{T_{c,ref}+273} \propto_{ref} \qquad (6)$$

d) Calculation of Series Resistance (Rs)

To calculate the series resistance, one must need,

$$R_S = \frac{\propto_{ref}\ln\left(1 - \frac{I_{mp,ref}}{I_{sc,ref}}\right) + V_{oc,ref} - V_{mp,ref}}{I_{mp,ref}} \qquad (7)$$

B. Modelling of DC-DC Converters

To provide symmetric input to MMI, the DC-DC converter in the solar photovoltaic conversion system is running at full power.

Equation (8) shows how the output voltage of the DC-DC boost up converter is dependent on the duty cycle.

$$V_{out} = \frac{V_{in}}{1-D} \qquad (8)$$

a) Design of an Inductor (L)

Following, using Equations (9) and (10), is the layout of the required Inductor for the system.

$$L_1 = \frac{V_{in}*(V_{out} - V_{in})}{\Delta I_L * f_s * V_{out}} \qquad (9)$$

$$\Delta I_L = (2\% - 4\%) * I_{out(\max)} * \frac{V_{out}}{V_{in}} \qquad (10)$$

b) Design of a Capacitor

Using Eqs. (11), and (12), we can see how the required Capacitor for the system should be designed.

$$C_1 = \frac{I_{(out)}*D}{f_s*\Delta V_{out}} \qquad (11)$$

$$\Delta V_L = (2\% - 4\%) * V_{out(max)} * \frac{I_{out}}{I_{in}} \qquad (12)$$

$V_{out\,(max)}$ is the maximum voltage delivered by the PV module under STC.

C. Design for Multilevel Inverter

As can be seen in Figure-2, the input voltage separator is made up of five sets of serially coupled solar PV modules labeled SPV1, SPV2, SPV3, SPV4, and SPV5. The H-bridge (Q1, Q2, Q3, and Q4) receives the input voltage after passing through a series of semiconductor devices (some regulated, some not) indicated as S1, S2, S3, S4, S5, D1, D2, D3, D4, and D5. The symmetrical modular multilevel structure dramatically expands the range of voltages that can be output, as shown by Equations (13) and (14).

VOL. 18, NO. 19, OCTOBER 2023 ISSN 1819-6608
ARPN Journal of Engineering and Applied Sciences

www.arpnjournals.com

$$N_{level} = 2S + 1 \quad (13)$$

$$N_{IGBT} = S + 4 \quad (14)$$

D. Design of Water Pump

An IM drive and centrifugal pump make up the maritime water pumping system. The "law of pump affinity" is often utilised as a principle while developing a centrifugal pump. According to Eq. (15), the load torque increases as the square of the speed.

$$T_L = k_p * \omega_r^2 \quad (15)$$

Where k_p=0.00043712Nm/(rad/sec)^2

3. SYSTEM DESCRIPTION AND PROPOSED STRATEGY

For maritime water pumping, the suggested system is a photovoltaic (PV) fed modular multilevel inverter (MMI) controlled by a PI, a fuzzy logic (FL) controller. An induction motor (IM) is controlled by the system to pump seawater at a steady rate.

A PV array, micro-miniature inverter, and inverter make up the system. The MMI receives direct current (DC) power that is generated by the PV array. To generate the necessary output voltage, the MMI architecture uses a series connection of several half-bridge submodules. PWM techniques are used to regulate the submodules, resulting in superior output waveforms.

To control the inverter and IM output, three distinct control strategies-PI control, FL control, and ANFIS control- are used. The PI controller is a time-tested method of control with numerous practical uses in industry. For complex systems, the FL controller's non-linear control approach is ideal. The performance of the controllers is evaluated using several robustness metrics, including peak overshoot, inverter settling time, and total harmonic distortion (THD). The suggested system is unusual because it combines the PV array, MMI, and intelligent controllers for the exclusive purpose of marine water pumping. The system's efficiency and performance can be enhanced by the implementation of modular multilevel inverters and intelligent control approaches. The system is adaptable for use in aquaculture, seawater desalination, and offshore oil drilling, among other marine water pumping applications.

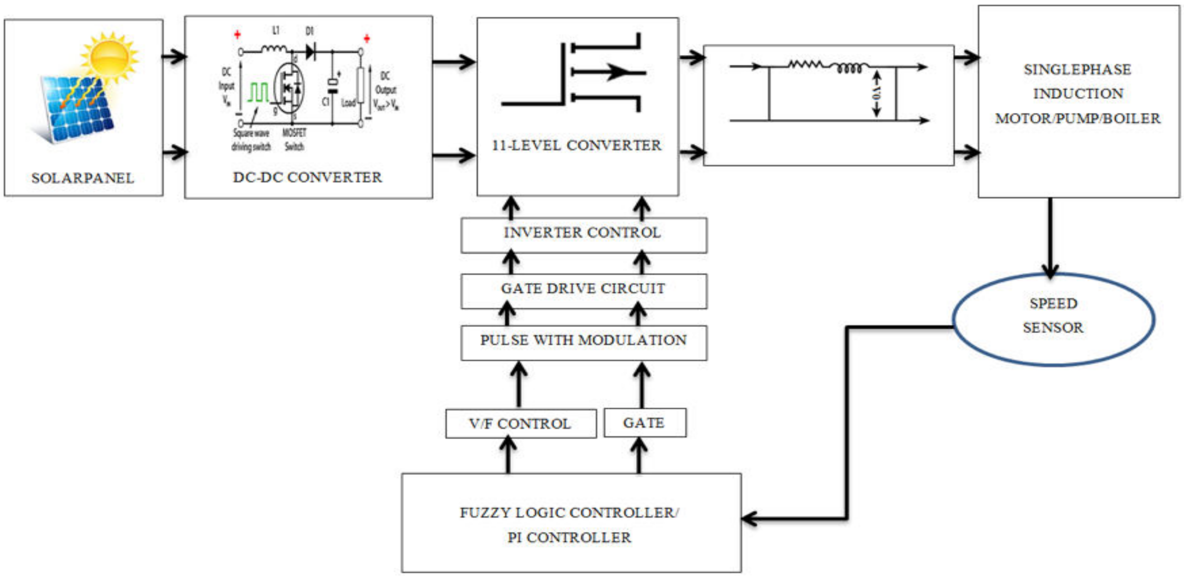

Figure-2. Proposed inverter.

VOL. 18, NO. 19, OCTOBER 2023 ISSN 1819-6608
ARPN Journal of Engineering and Applied Sciences

www.arpnjournals.com

4. COMPONENTS USED

Solar Panel	>Diode-0.001 ohms(Resistance ron) >IGBT-1e-3 ohms(Internal resistance) >Pulse Generator-40(pulse width)
PID Controller	>Propotional-1 >Integral-1 >Derivative-0 >Filter Coefficient-100 >Time Domain - Continuous
Mosfet	>FET resistance Ron-0.1 ohms >Internal Diode Inductance lon-0 H >Internal Diode Resistance-0.01 ohms >Snubber Resistance-1e5 ohms
Diode	>Resistance Ron-0.001 ohms >Inductance Lon-0 H >Forward Voltage VF-0.8 V >Snubber Resistance-500 ohms

A. PI Controller

Commonly employed in industrial control systems is a form of feedback controller known as a proportional-integral controller (PI controller). It functions by modifying the input to a system based on the current and past differences between the desired and actual outputs of that system.

The controller's proportional term responds to the system's current error (the gap between the desired and actual output) by adjusting the input accordingly. The integral term accounts for the error's past, which helps to get rid of it in the system's steady state. By adjusting the input based on both the current error and the history of error, the PI controller can help a system achieve a more accurate and stable output.

System performance can be improved with careful selection of controller gains for the proportional and integral terms. A system can become unstable and experience oscillations around the targeted output if the proportional gain is too large. The system can become sluggish and slow to respond to changes in the desired output if the integral gain is too large. Finding the right balance between these two terms is crucial for the performance of the PI controller.

A.1 Simulation Results Using Pi Controller

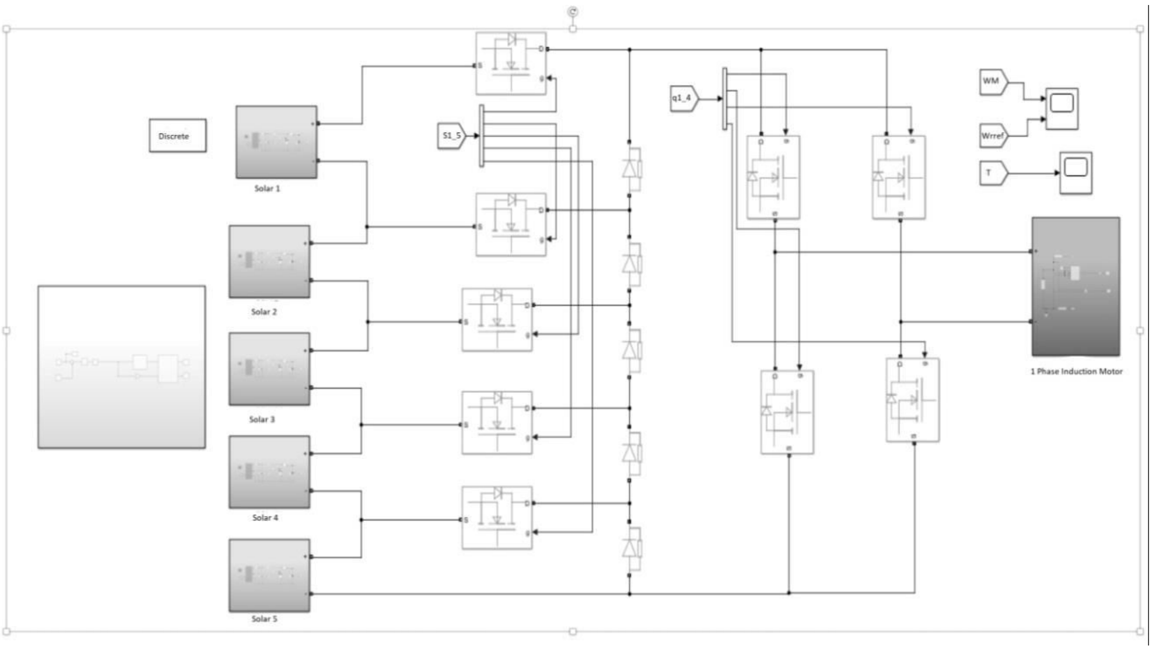

Figure-3. Schematic diagram using pi controller.

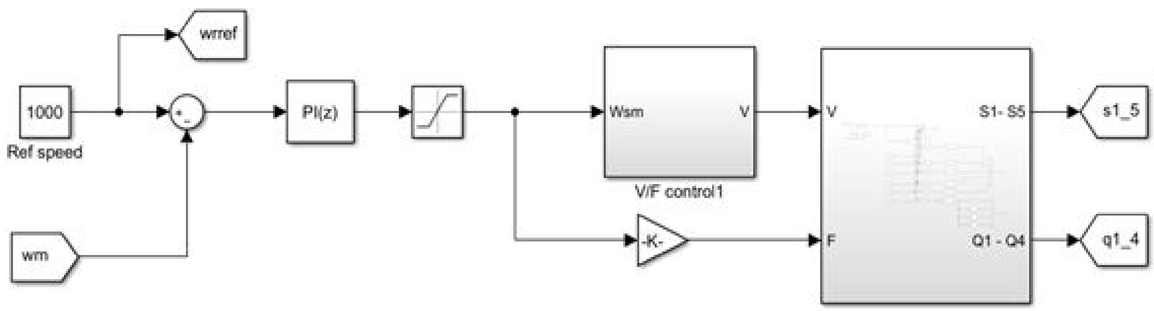

Figure-4. Controlling part of the pi controller.

VOL. 18, NO. 19, OCTOBER 2023 ISSN 1819-6608
ARPN Journal of Engineering and Applied Sciences

www.arpnjournals.com

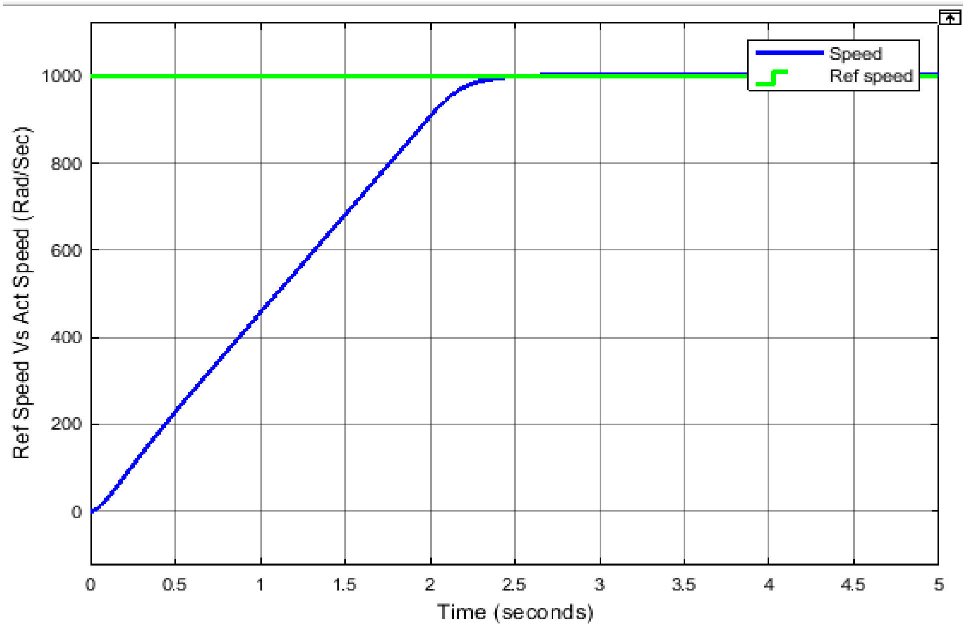

Figure-5. Ref speed and actual speed of the pi controller.

The reference speed of the motor operated through the PI controller is 1000 Rad/Sec whereas the actual speed starts from 0 Rad/Sec and gradually increases to reference speed with a period of 2.343 sec and maintains a steady state from there to operation.

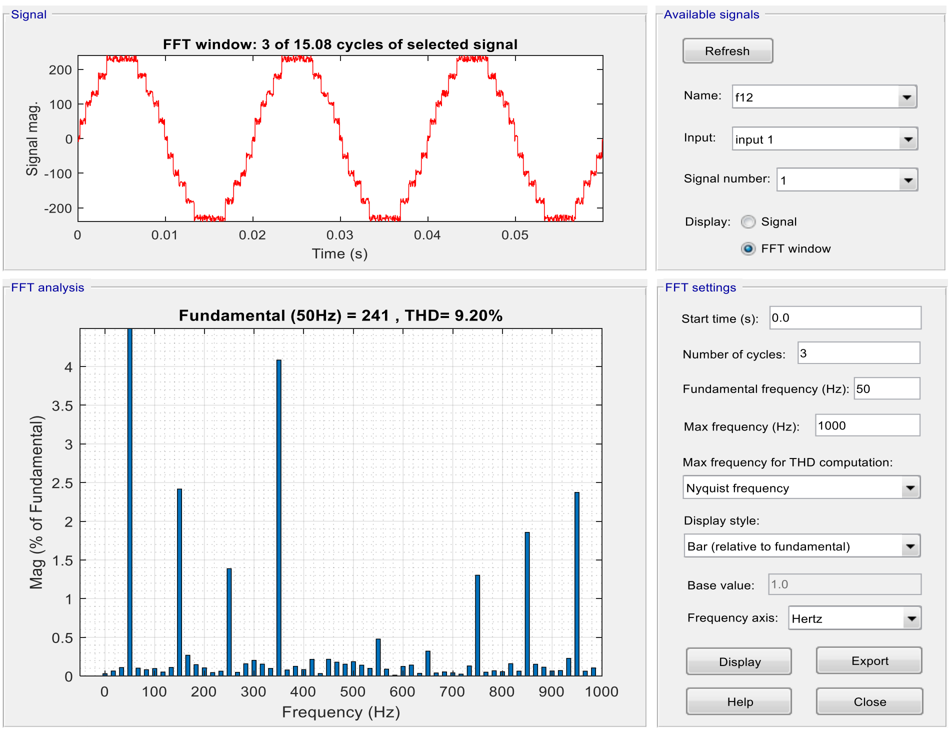

Figure-6. THD using a Pi controller.

The THD (Total Harmonic Distortion) was at 9.20% when it was operated with a Pi controller which was used in the conventional systems.

B. Fuzzy Controllers

Fuzzy logic is a mathematical technique for dealing with imprecise or uncertain data, and it is employed in a specific kind of controller called a fuzzy controller. Input variables, such as temperature or pressure, are mapped onto fuzzy sets, which are

ARPN Journal of Engineering and Applied Sciences

characterised by language variables such as "hot," "cold," "high," or "low." This allows the controller to perform its function.

To arrive at useful output values, the fuzzy controller applies rules derived from these fuzzy sets. Experts or machine learning algorithms often define or develop these rules. Additionally, the output values are fuzzy sets that are defuzzified to yield a clean value that can be used to regulate the regulated system.

Fuzzy controllers excel in real-world applications due to their ability to deal with imprecise or uncertain data. For instance, if the process temperature shifts over time, the output of a fuzzy controller can be tuned to account for this.

Process control, robotics, and automotive systems are just a few examples of where you can find a fuzzy controller in use. To boost performance or give more stable control, they can be integrated with other controller types like PI or PID controllers.

The input to the fuzzy operator is a set of relationship values derived by the fuzzifier. One truth value is returned as the result. The mistake is always represented by Input 1, but any updates to the error are shown by Input 2. There are eight fuzzy groups of linguistic variables, of which five are described here.

a) Big negative error speed (NB)

b) Small negative error speed (NS)

c) Small positive error speed (PS)

d) Positive error speed Big (PB)

e) Zero error speed (ZE).

Table 1. Fuzzy Rules.

e/ce	NB	NS	ZE	PS	PB
NB	ZE	NS	NB	NB	NB
NS	ZE	NS	NB	NS	NB
ZE	PB	PS	ZE	NS	NB
PS	PB	PS	PS	ZE	NS
PB	PB	PB	PB	PS	ZE

The FLC table consists of rows and columns. Each row represents a rule, and each column corresponds to a linguistic variable or membership function associated with the input and output variables of the fuzzy logic controller.

B.1. Simulation Results Using Fuzzy Logic Controller

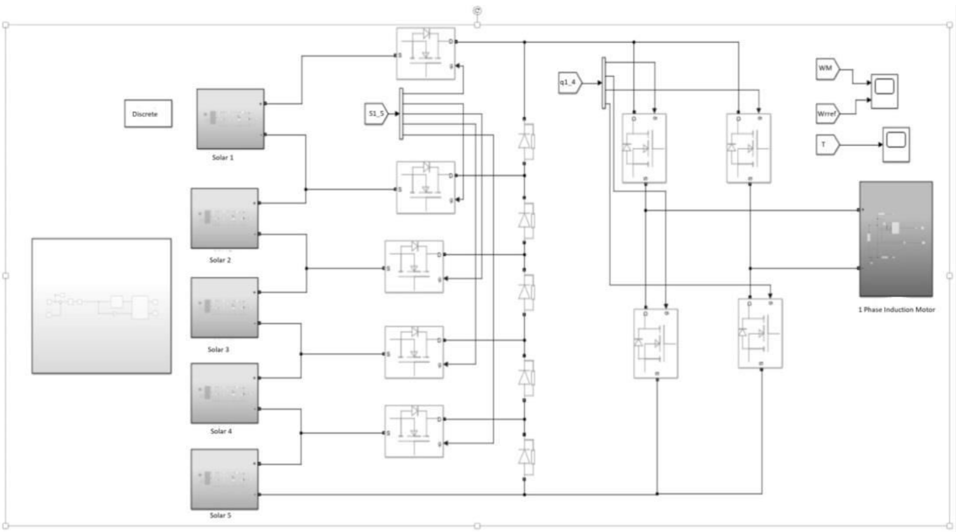

Figure-7. Schematic diagram using a fuzzy logic controller.

ARPN Journal of Engineering and Applied Sciences

www.arpnjournals.com

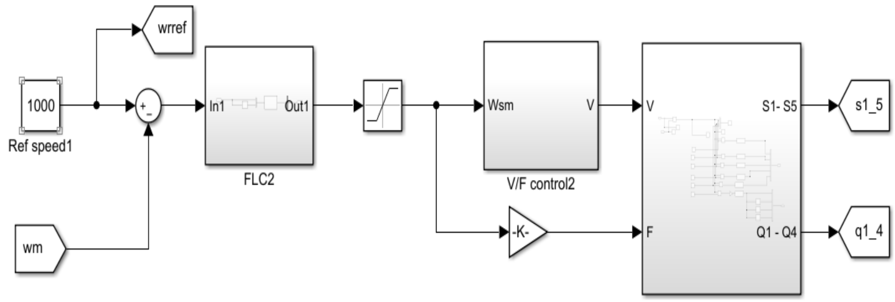

Figure-8. Controlling part of the fuzzy logic controller.

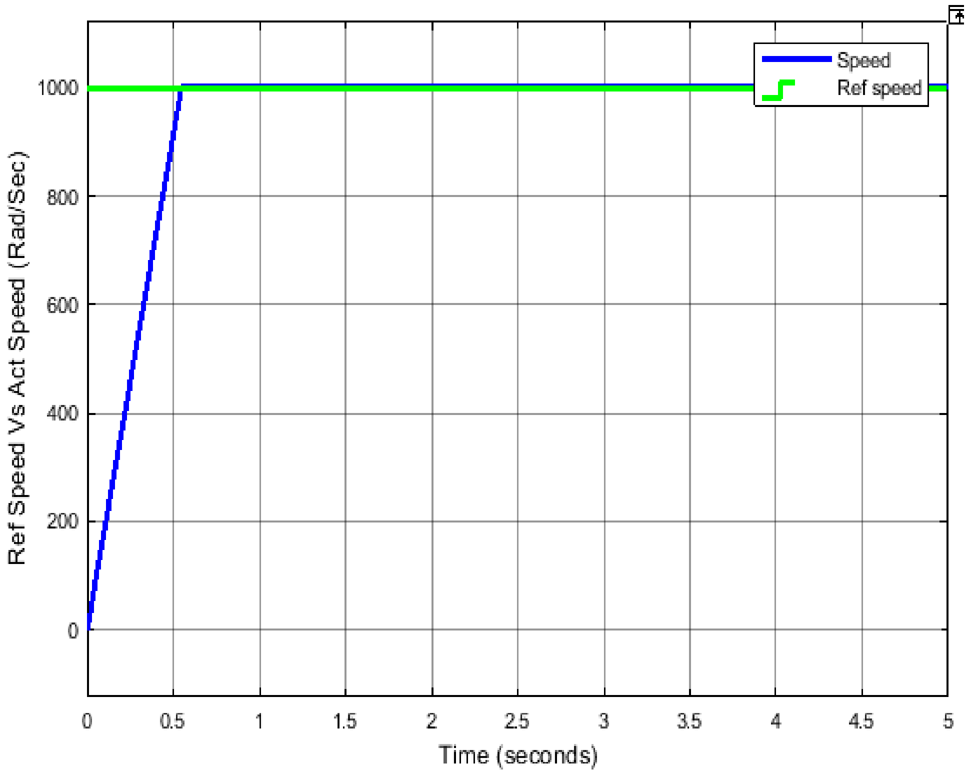

Figure-9. Ref speed and actual speed of the fuzzy logic controller.

The reference speed of the motor operated through the Fuzzy logic controller is 1000 Rad/Sec whereas the actual speed starts from 0 Rad/Sec and gradually increases to reference speed with a period of 0.623 sec and maintains a steady state from there to maintain the speed for the motor.

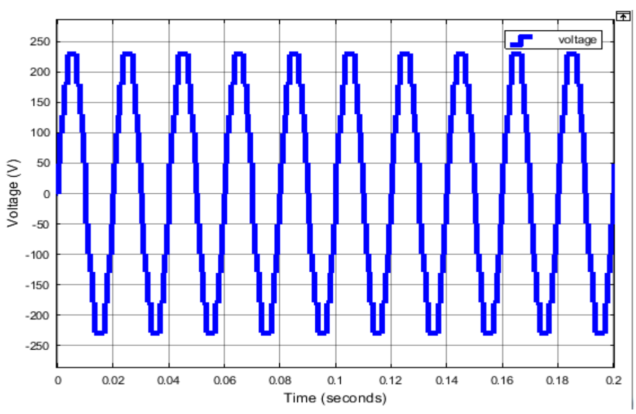

Figure-10. 11 Level Voltage using a fuzzy logic controller.

VOL. 18, NO. 19, OCTOBER 2023 ISSN 1819-6608
ARPN Journal of Engineering and Applied Sciences

www.arpnjournals.com

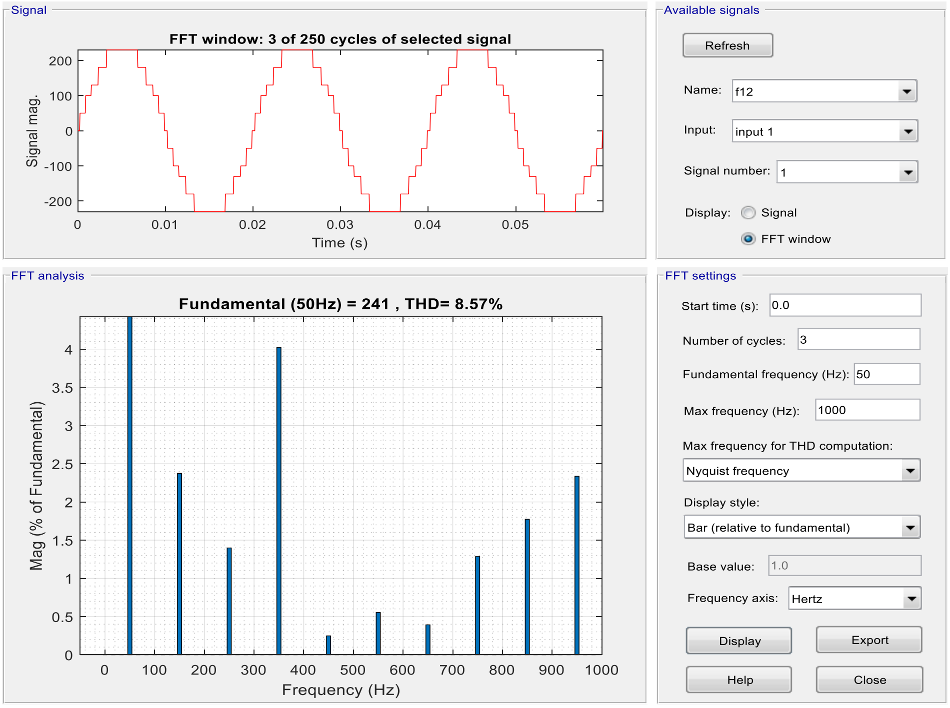

Figure-11. THD uses a fuzzy logic controller.

The THD (Total Harmonic Distortion) was reduced to 8.57% when it was operated with a Fuzzy logic controller instead of using a Pi controller.

5. ANALYSIS TAB LE OF SIMULATION RESULT

Comparative THD using PI and fuzzy logic controller is shown in Figure-12 and values are indicated in Table-2.

Table-2. Comparative THD using PI and fuzzy logic controller.

Controller Type	Total harmonic distortion	Time(sec)
PI Controller	9.20%	2.343
Fuzzy Controller	8.57%	0.623

ARPN Journal of Engineering and Applied Sciences

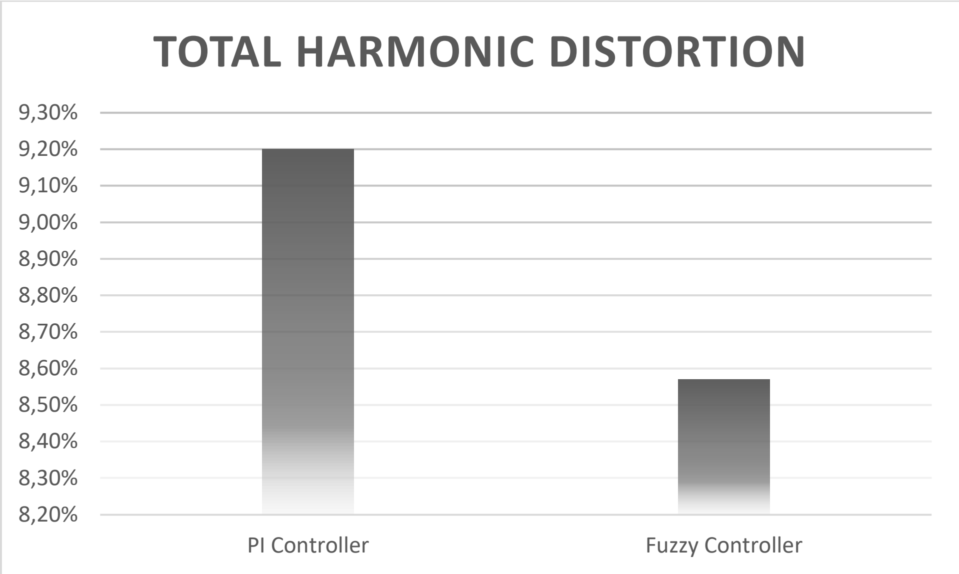

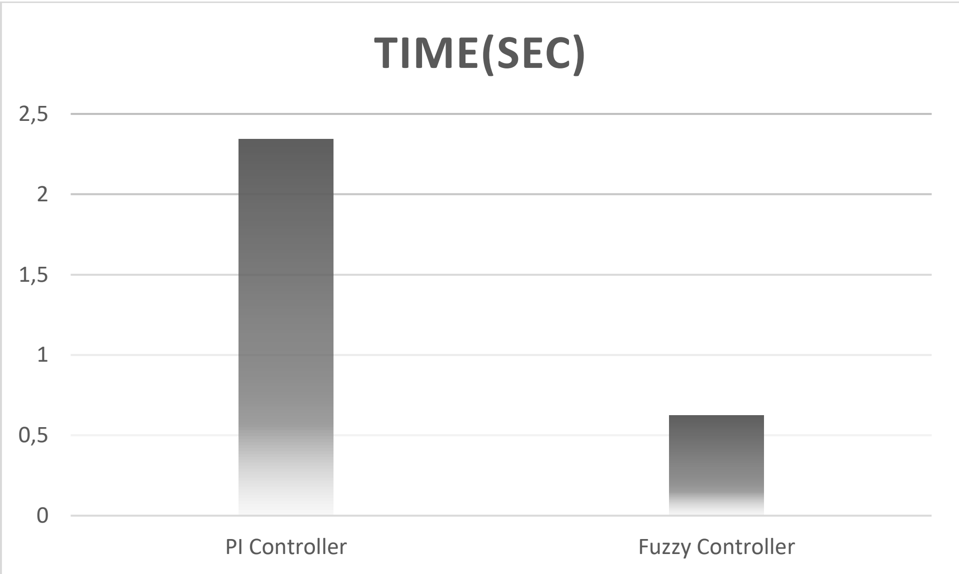

Figure-12. Comparative THD using PI and fuzzy logic controller.

6. CONCLUSIONS

This study explains how a Modular Multilevel Inverter (MMI) with advanced ways of managing the Induction Motor (IM) drive was built for pumping seawater. The steady-state and dynamic behaviours of an MMI driven by solar PV were measured to determine the device's practicality for controlling the speed of an induction motor drive in a maritime water pumping system. A photovoltaic (PV) array is used to power an induction motor with the help of the proposed inverter. Feedback from the motor's speed is used by the controller to provide the most efficient PWM pulses for the inverter switches. Using PI, FL, the motor is started slowly and its speed is gradually increased to the reference speed. We verify the PI, FL, and anfis controllers' performance is enough for practical implementation by comparing the simulation results. The results show that compared to the PI controller, the Fuzzy logic controller has a shorter settling time and produces fewer harmonics. Both the steady-state inaccuracy of the induction motor speed control and the harmonics of the modular multilevel inverter's output voltage are positively affected by the proposed control method.

REFERENCES

[1] H. Lan, Y. Bai, S. Wen, D. C. Yu, Y.-Y. Hong, J. Dai and P. Cheng. 2016. Modeling and stability analysis of hybrid PV/diesel/ESS in ship power system Inventions, 1(5): 1-16, doi: 10.3390/inventions1010005.

[2] S. G. Jayasinghe, L. Meegahapola, N. Fernando, Z. Jin and J. M. Guerrero. 2017. Review of ship microgrids: System architectures, storage

technologies and power quality aspects. Inventions, 2(4): 1-19, doi: 10.3390/inventions2010004.

[3] R. Kumar and B. Singh. 2017. Single stage solar PV fed brushless DC motor driven water pump. IEEE J. Emerg. Sel. Topics Power Electron., 5(3): 1337-1385, doi: 10.1109/JESTPE.2017.2699918.

[4] S. Shukla and B. Singh. 2018. Single-stage PV array fed speed sensorless vector control of induction motor drive for water pumping. IEEE Trans. Ind. Appl., 54(4): 3575-3585, doi: 10.1109/TIA.2018.2810263.

[5] C.-L. Su, W.-L. Chung and K.-T. Yu. 2014. An energy-savings evaluation method for variable-frequency-drive applications on ship central cooling systems. IEEE Trans. Ind. Appl., 50(2): 1286-1297, doi: 10.1109/TIA.2013.2271991.

[6] B. Singh, U. Sharma, and S. Kumar. 2018. Standalone photovoltaic water pumping system using induction motor drive with reduced sensors. IEEE Trans. Ind. Appl., 54(4): 3645-3655, doi: 10.1109/TIA.2018.2825285.

[7] A. Dolatabadi and B. Mohammadi-Ivatloo. 2018. Stochastic risk-constrained optimal sizing for hybrid power system of merchant marine vessels. IEEE Trans. Ind. Informat., 14(12): 5509-5517, doi: 10.1109/TII.2018.2824811.

[8] H.-L. Tsai. 2014. Design and evaluation of a photovoltaic/thermal-assisted heat pump water heating system. Energies, 7(5): 3319-3338, doi: 10.3390/en7053319. 88532 VOLUME 9, 2021 A. Alexander Stonier et al.: FL Control for Solar PV Fed MMI

[9] M. G. Yu, Y. Nam, Y. Yu, and J. Seo. 2016. Study on the system design of a solar assisted ground heat pump system using dynamic simulation. Energies, 9(4): 1-17, doi: 10.3390/en9040291.

[10] S. V. Giannoutsos and S. N. Manias. 2015. A systematic power-quality assessment and harmonic filter design methodology for variable-frequency drive application in marine vessels. IEEE Trans. Ind. Appl., 51(2): 1909-1919, doi: 10.1109/TIA.2014.2347453.

[11] C. Gnanavel and S. A. Alexander. 2018. Experimental validation of an eleven level symmetrical inverter using genetic algorithm and queen bee assisted genetic algorithm for solar photovoltaic applications. J. Circuits, Syst. Comput., 27(13): 1-23, doi: 10.1142/S0218126618502122.

[12] R. Thangaraj, T. R. Chelliah, M. Pant, A. Abraham, and C. Grosan. 2011. Optimal gain tuning of PI speed controller in induction motor drives using particle swarm optimization. Log. J. IGPL, 19(2): 343-356, doi: 10.1093/jigpal/jzq031.

[13] M. S. Zaky and M. K. Metwaly. 2017. A performance investigation of a four-switch three-phase inverter-fed IM drives at low speeds using fuzzy logic and PI controllers. IEEE Trans. Power Electron., 32(5): 3741-3753, doi: 10.1109/TPEL.2016.2583660.

[14] R. E. Geneidy, K. Otto, P. Ahtila, P. Kujala, K. Sillanpää and T. Mäki-Jouppila. 2018. Increasing energy efficiency in passenger ships by novel energy conservation measures. J. Mar. Eng. Technol., 17(2): 85-98, doi: 10.1080/20464177.2017.1317430.

[15] A. A. Stonier. 2017. Design and development of high performance solar photovoltaic inverter with advanced modulation techniques to improve power quality. Int. J. Electron. 104(2): 174-189.